Accepted Manuscript

Design, synthesis and anti-HIV evaluation of novel diarylpyridine derivatives as potent HIV-1 NNRTIs

Zhaoqiang Liu, Ye Tian, Jinghan Liu, Boshi Huang, Dongwei Kang, Erik De Clercq, Dirk Daelemans, Christophe Pannecouque, Peng Zhan, Xinyong Liu

PII: S0223-5234(17)30534-2

DOI: 10.1016/j.ejmech.2017.07.012

Reference: EJMECH 9575

To appear in: *European Journal of Medicinal Chemistry*

Received Date: 27 January 2017

Revised Date: 6 July 2017

Accepted Date: 9 July 2017

Please cite this article as: Z. Liu, Y. Tian, J. Liu, B. Huang, D. Kang, E. De Clercq, D. Daelemans, C. Pannecouque, P. Zhan, X. Liu, Design, synthesis and anti-HIV evaluation of novel diarylpyridine derivatives as potent HIV-1 NNRTIs, *European Journal of Medicinal Chemistry* (2017), doi: 10.1016/j.ejmech.2017.07.012.

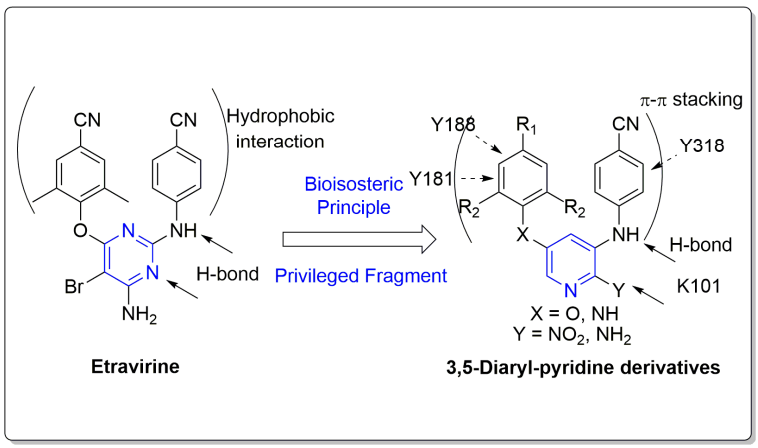

Etravirine **3,5-Diaryl-pyridine derivatives**

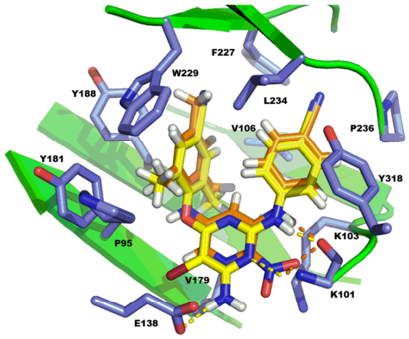

5b2 (Orange)
R_1 = CN, R_2 = CH_3, X = NH, Y = NO_2;
$EC_{50\ IIIB}$ = 0.04 μM; SI = 3963.

Design, synthesis and anti-HIV evaluation of novel diarylpyridine derivatives as potent HIV-1 NNRTIs

Zhaoqiang Liu[1,a], Ye Tian[1,a], Jinghan Liu[b], Boshi Huang[a], Dongwei Kang[a], Erik De Clercq[c], Dirk Daelemans[c], Christophe Pannecouque[c], Peng Zhan[*,a], Xinyong Liu[*,a]

[a]*Department of Medicinal Chemistry, Key Laboratory of Chemical Biology (Ministry of Education), School of Pharmaceutical Sciences, Shandong University, 44, West Culture Road, 250012, Jinan, Shandong, P.R. China;*

[b]*Shool of life science and technology, China Pharmaceutical University, 639 Longmian Avenue, 210009, Nanjing, P.R. China;*

[c]*Rega Institute for Medical Research, KU Leuven, Minderbroedersstraat 10, B-3000 Leuven, Belgium*

Abstract

As a continuation of our efforts to discover and develop “me-better” drugs of DAPYs, novel diarylpyridine derivatives were designed, synthesized and evaluated for their anti-HIV activities in MT-4 cells. The majority of these compounds showed high activity against wild-type HIV-1 strain (IIIB) with EC_{50} values in the range of 0.04-4.41 μM. Among them, compound **5b2** (EC_{50} = 0.04 μM, SI = 3963) was the most potent. This compound showed anti-HIV-1_{IIIB} activity superior than of Nevirapine but still inferior than of Etravirine. Selected compounds were also evaluated for the activity against reverse transcriptase (RT), and most of the compounds exhibited submicromolar IC_{50} values indicating they are specific RT inhibitors. Preliminary structure-activity relationships and modeling studies of these new analogues provide valuable avenues for future molecular optimization.

Keywords: *HIV-1; NNRTIs; pyridine; bioisosteric principle; drug design*

[*] Corresponding authors. Tel: +86-531-88380270; Fax: +86-531-88382731; E-mail: zhanpeng1982@sdu.edu.cn (P. Zhan), xinyongl@sdu.edu.cn (X. Liu).

[1] Zhaoqiang Liu and Ye Tian contributed equally to this article.

1. Introduction

HIV-1 non-nucleoside reverse transcriptase inhibitors (NNRTIs) are essential components of highly active antiretroviral therapy (HARRT) due to their excellent potency, remarkable selectivity and relatively low toxicity. Nevertheless, the unavoidable emergence of drug-resistant viruses and severe side effects associated with the long-term administration of the clinical approved NNRTIs demand unremitting efforts to discover novel NNRTIs candidates with different resistance profiles and improved drug-like properties [1-3].

Among more than 50 different series of NNRTIs that have been reported [3-5], diarylpyrimidine (DAPY) derivatives, as second generation NNRTIs, have attracted considerable attention over the past few years due to their potent activity against wild and various mutant HIV-1 strains. Two DAPY derivatives, Etravirine (TMC125, ETR) and Rilpivirine (TMC278, RPV), have been approved by FDA for the treatment of HIV infection in 2008 and 2011 respectively (**Fig. 1**). However, newly reported adverse effects of ETR and RPV [6] along with the imperfect pharmacokinetics profiles of the most DAPY derivatives [7, 8] encouraged researches on exploring novel NNRTI agents with better drug-like properties for the treatment of HIV infections [4]. According to the results obtained from crystallography [9] and structure-activity relationship (SAR) [10, 11] studies, this central pyrimidine ring of DAPY derivatives is tolerant for isosteric replacement. In our previous studies [12-18], replacement of the central pyrimidine ring using structure-based drug design and bioisosteric principle had led to the discovery of novel series of potent NNRTIs, such as pyridazine derivatives [17] and 2-pyridone derivatives [18], which are proved to be highly effective in inhibiting HIV-1 replication.

As an extension of these investigations and with the aim to generate novel NNRTIs with desirable potency and drug-like properties, novel diarylpyridine derivatives were designed via replacing the pyrimidine core present in DAPY derivatives by the bioisosteric pyridine which is one of the heterocycles with significant and privileged bioactivity and pharmacokinetic properties [19]. In the target structures, the active para-cyanoaniline moiety was retained, along with various substituents at the 5-position of the central pyridine as the left wing of the structure. Besides, we incorporated a nitro or amino group at the 2-position on the pyridine ring trying to provide a stronger H-bonding with the lysine 101 (K101) of the viral enzyme RT, as either an H-bond

acceptor or donor, than the nitrogen on the original pyrimidine ring of TMC125 (**Fig. 1**). Herein, we report the synthesis, anti-HIV evaluation and preliminary SAR of these diarylpyridine derivatives.

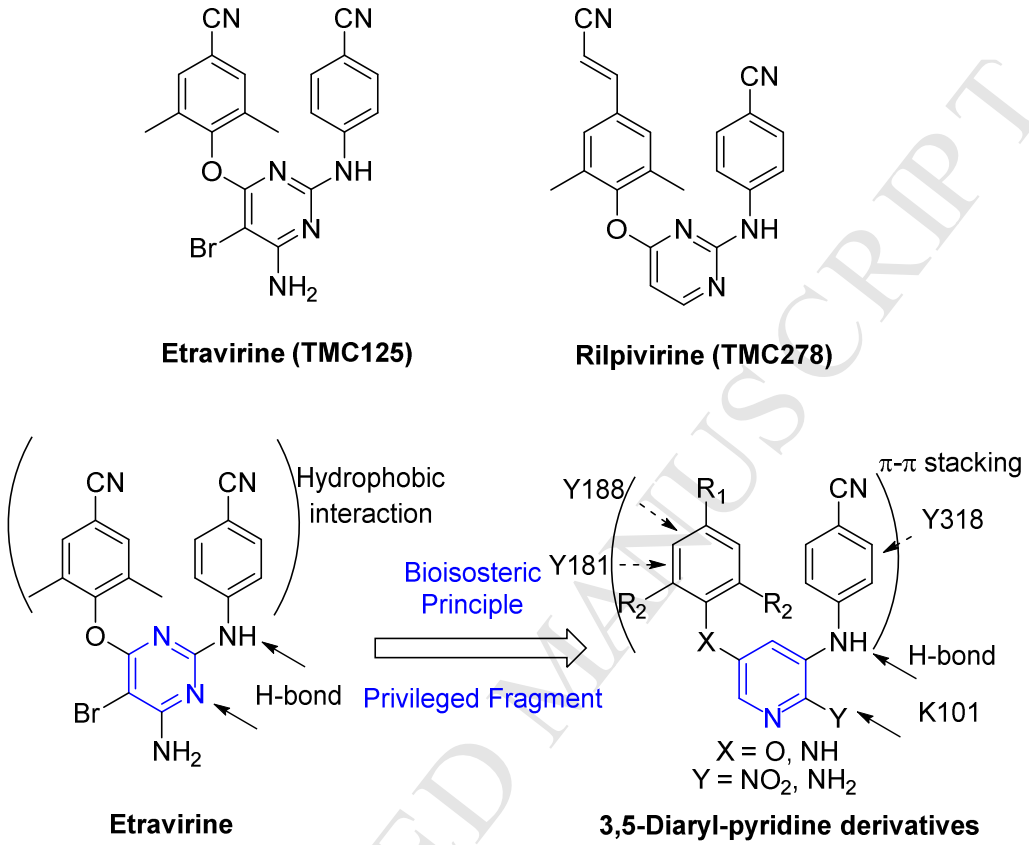

Figure 1. FDA approved DAPYs as NNRTIs and the design of novel diarylpyridine derivatives

2. Results and discussion

2.1. Chemistry

The newly designed diarylpyridine derivatives were synthesized straightforwardly [20] as depicted in **Scheme 1**. Reaction of commercially available 3-amino-5-bromopyridine with propyl chlorocarbonate afforded propyl (5-bromopyridin-3-yl)carbamate (**1**). The regioselective nitration of **1** [21] in the presence of HNO_3/H_2SO_4, resulted in the formation of propyl (5-bromo-2-nitropyridin-3-yl)carbamate **2** whose hydrolysis, using KOH-EtOH-H2O, afforded 5-bromo-2-nitropyridin-3-amine (**3**). Buchwald-Hartwig reaction of **3** with 4-aminobenzonitrile gave 4-((5-bromo-2-nitropyridin-3-yl)amino)benzonitrile (**4**). Then derivatives **5a1-10** were obtained from **4** by Ullman condensation with different substituted phenols, while **5b1-2** were

obtained by Buchwald-Hartwig reaction with appropriate anilines. Further treatment of **5a1-9** with $SnCl_2 \cdot 2H_2O$ gave compounds **6a1-9**.

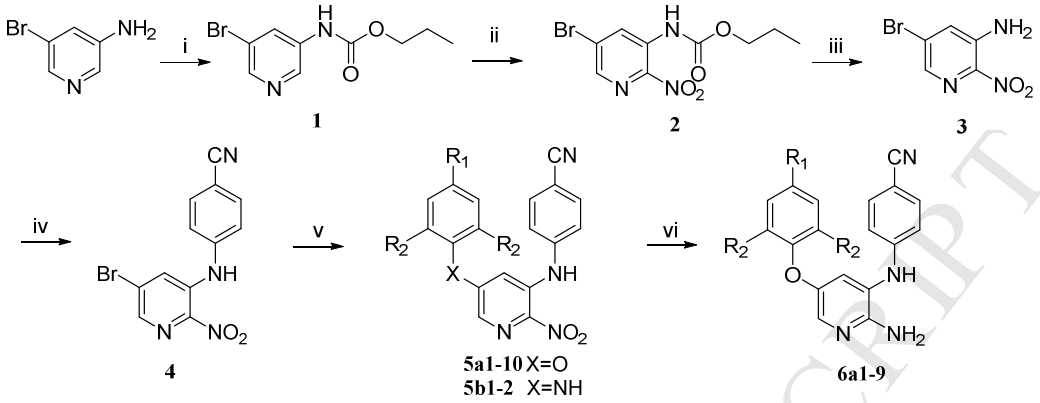

Scheme 1. Reagents and conditions: i: Propyl chlorocarbonate, $NaHCO_3$; ii: H_2SO_4-HNO_3; iii: KOH, H_2O-EtOH; iv: 4-aminobenzonitrile, palladium acetate, Xantphos, Cs_2CO_3, 90 °C; v: ArOH, CuI, picolinic acid, K_3PO_4, 90 °C or $ArNH_2$, palladium acetate, Xantphos, Cs_2CO_3, 90 °C; vi: $SnCl_2 \cdot 2H_2O$, EtOH, reflux.

2.2. Anti-HIV activity evaluation

The newly synthesized diarylpyridine derivatives were evaluated for anti-HIV activity against wild-type (wt) HIV-1 strain (IIIB), K103N+Y181C double mutant HIV-1 strain (RES056) and HIV-2 strain (ROD) in MT-4 cells using the MTT method [22-24]. Nevirapine (NVP), Zidovudine (azidothymidine, AZT), Efavirenz (EFV) and Etravirine were used as reference drugs. The cytotoxicity of these compounds was determined in parallel. The results, expressed as EC_{50}, CC_{50} and SI, are illustrated in **Table 1**.

Table 1. Activity and cytotoxicity of the title compounds in MT-4 cells.

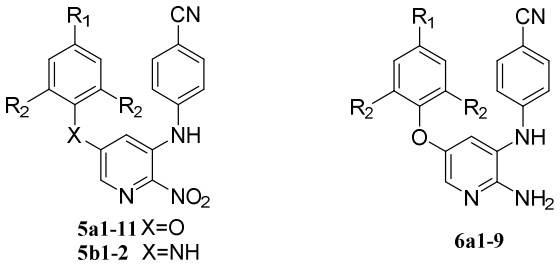

Compds	R_1	R_2	EC_{50} (μM)[a]	CC_{50} (μM)[b]	SI

			IIIB	ROD	RES056		(IIIB)[c]
5a1	CN	CH_3	4.12 ± 0.55	>324.4	>324.4	>324.4	>79
5a2	CH_3	CH_3	0.29 ± 0.024	>333.9	>333.9	>333.9	>1161
5a3	CH_3	Br	0.0 5± 0.003	>84.34	>84.34	84.34 ± 19.36	1678
5a4	H	CH_3	2.03 ± 0.36	>346.9	>346.9	>346.9	>171
5a5	H	OCH_3	>318.6	>318.6	-	>318.6	X1[d]
5a6	Cl	CH_3	1.41 ± 0.42	>316.6	>316.6	>316.6	>171
5a7	Br	CH_3	4.41 ± 1.14	>284.6	>284.6	>284.6	>64
5a8	Cl	Cl	0.31 ± 0.049	>286.9	>286.9	>286.9	>924
5a9	Br	Br	0.79 ± 0.19	>219.7	>219.7	>219.7	>277
5a10	F	F	1.01 ± 0.16	>323.6	>323.6	>323.6	>320
5b1	H	CH_3	1.06 ± 0.20	>6.27	>6.27	6.27 ± 0.34	6
5b2	CH_3	CH_3	0.04 ± 0.006	>167.7	>167.7	167.7 ± 56.32	3963
6a1	CN	CH_3	0.07 ± 0.015	>39.53	⩾11.45	39.53 ± 6.97	577
6a2	CH_3	CH_3	0.14 ± 0.028	>32.09	>32.09	32.09 ± 4.05	227
6a3	CH_3	Br	0.07 ± 0.02	>263.6	>263.6	>263.6	>3803
6a4	H	CH_3	0.60 ± 0.28	>378.3	>378.3	>378.3	>628
6a5	H	OCH_3	35.73 ± 6.83	>344.9	>344.9	>344.9	>10
6a6	Cl	CH_3	0.37 ± 0.14	>35.06	>35.06	35.06 ± 13.26	95
6a7	Br	CH_3	0.84 ± 0.32	>26.68	>26.68	26.68 ± 0.53	32
6a8	Cl	Cl	0.26 ± 0.02	⩾57.68	>178.6	178.6 ± 85.58	680
6a9	Br	Br	0.50 ± 0.14	>27.68	>27.68	27.68 ± 9.05	55

NVP	0.25 ± 0.066	-	>15.02	>15.02	>60
EFV	0.005 ± 0.002	-	0.31 ± 0.16	>6.34	>1258
ETR	0.004 ± 0.0002	-	0.017 ± 0.002	>4.59	>1128
AZT	0.006 ± 0.002	-	0.011 ± 0.005	>7.48	>1288

[a]EC_{50}: concentration of compound required to achieve 50% protection of MT-4 cell cultures against HIV-1-induced cytotoxicity, as determined by the MTT method.

[b]CC_{50}: concentration required to reduce the viability of mock-infected cell cultures by 50%, as determined by the MTT method.

[c]SI: selectivity index, the ratio of CC_{50}/EC_{50}.

[d]X1: stands for $\geqslant$ 1 or <1.

The majority of the synthesized compounds showed high activities against wt HIV-1 strain (IIIB) with EC_{50} values in the range of 0.04-4.41 μM. Totally, 4 compounds were found more potent than the reference drug NVP (EC_{50} = 0.25 μM) against wt HIV-1. They are **5a3** (EC_{50} = 0.05 μM), **6a1** (EC_{50} = 0.07 μM), **6a3** (EC_{50} = 0.07 μM) and the most effective **5b2** with an EC_{50} value of 0.04 μM, which was about 6 times more potent than NVP. Unfortunately, these compounds were still less active than other tested control drugs, *i.e.* EFV (EC_{50} = 0.005 μM), ETR (EC_{50} = 0.004 μM) and AZT (EC_{50} = 0.006 μM). For example, **5b2** was about 10 times less active than ETR.

Most compounds showed low cytotoxicity, and 12 out of them had CC_{50} > 200 μM. Taken the safety profile into consideration, compounds **5b2** and **6a3** with the largest SI (= 3963 or > 3807, respectively) were the best two compounds in this series.

The contribution of the 2-pyridine substituent (NH_2 or NO_2) to the biological activity was firstly determined. Except for **5a3** and **6a3**, the compounds of the **6a** sub-series (NH_2 at the 2 position of the pyridine ring) showed better activity than those of **5a** sub-series (NO_2 group at the 2 position of the pyridine ring). This result suggests that the hydrogen bond donor/acceptor properties of the NH_2 group were better than the hydrogen bond acceptor properties of the NO_2. However, the NH_2 moiety contributes more than the NO_2 to the cytotoxicity because most of the compounds in **6a** sub-series are more toxic than their counterparts in **5a** sub-series.

Next, we turned the attention to the SAR on the left ring, the compounds substituted with anilines (X = NH) at the 5 position of the pyridine ring (**5b1**, EC_{50} = 1.06 μM; **5b2**, EC_{50} = 0.04 μM) were more potent than their counterparts with phenols (X= O) (**5a4**, EC_{50} = 2.03 μM; **5a2**, EC_{50} = 0.29 μM). However, compounds **5b1**, **5b2** were also more cytotoxic than **5a4**, **5a2**.

Within **5a** sub-series (X = O), compound **5a3** (R_1 = CH_3, R_2 = Br) is the most active. When R_2 = CH_3, a clear order of R_1 substituents for anti-HIV-1 activity was observed by comparison: CH_3 (**5a2**, EC_{50} = 0.29 μM) > Cl (**5a6**, EC_{50} = 1.41 μM) > H (**5a4**, EC_{50} = 2.03 μM) > CN (**5a1**, EC_{50} = 4.12 μM) > Br (**5a7**, EC_{50} = 4.41 μM).

In **6a** sub-series, the order of R_1 substituents when R_2 = CH_3 is slightly different: CN (**6a1**, EC_{50} = 0.07 μM) > CH_3 (**6a2**, EC_{50} = 0.14 μM) > Cl (**6a6**, EC_{50} = 0.37 μM) > H (**6a4**, EC_{50} = 0.60 μM) > Br (**6a7**, EC_{50} = 0.84 μM).

In both **5a** and **6a** series, the anti-HIV-1 activity of the compounds was influenced by the substituents at R_2 position as well. When the R_1 group was fixed, there were some interesting aspects related with the influence of R_2 on the activity which might reveal more SAR information. Thus, when R_1 = CH_3, compounds in which R_2 = Br (**5a3**, EC_{50} = 0.05 μM; **6a3**, EC_{50} = 0.07 μM) showed better activity than those having R_2 = CH_3 (**5a2**, EC_{50} = 0.29 μM; **6a2**, EC_{50} = 0.14 μM); when R_1 = H, compounds in which R_2 = OCH_3 (**5a3**, EC_{50} > 318.6 μM; **6a3**, EC_{50} = 35.73 μM) were significantly less active than those with R_2 = CH_3 (**5a4**, EC_{50} = 2.03 μM; **6a4**, EC_{50} = 0.60 μM); when R_1 = Cl, compounds in which R_2 = Cl (**5a8**, EC_{50} = 0.31 μM; **6a8**, EC_{50} = 0.26 μM) showed better activity than those with R_2 = CH_3 (**5a6**, EC_{50} = 1.41 μM; **6a6**, EC_{50} = 0.37 μM); when R_1 = Br, compounds in which R_2 = Br (**5a9**, EC_{50} = 0.79 μM; **6a9**, EC_{50} = 0.50 μM) showed better activity than those with R_2 = CH_3 (**5a7**, EC_{50} = 4.41 μM; **6a7**, EC_{50} = 0.84 μM). In general, comparing to CH_3, Br and Cl appeared to be advantageous substituents for the activity (*e.g.*, **5a3** and **6a8**), while the bulky methoxy group at this position led to a significant loss of antiviral potency (*e.g.*, **5a5**).

Finally, all the compounds lack potency against the double mutant strain RES056. In addition, none of the compounds showed inhibition of HIV-2 (ROD), which suggested these derivatives was specific for HIV-1.

2.3. HIV-1 RT inhibition assay

Eleven selected compounds were tested in enzymatic assays against wt HIV-1 RT using poly(rA)-oligo$(dT)_{16}$ as template/primer in order to confirm the binding target [25-27]. Nevirapine NVP and EFV were used as reference drugs (**Table 2)**. Except for **6a5**, all the compounds exhibited good inhibitory activity against wt HIV-1 RT with IC_{50} values in the range of 0.05-0.91 μM, which was greater than that of NVP (IC_{50} = 2.32 μM), comparable to that of EFV (IC_{50} = 0.04 μM), but still 4 times lower than ETR (IC_{50} = 0.01 μM). Among them, compound **6a3** exhibited the highest enzymatic inhibition activity, which was about 45 times higher than that of NVP. The results suggest that these diarylpyridine derivatives bind to HIV-1 RT and belong to the HIV-1 NNRTIs class. Basically, it reflected some SAR found in cell-based assay, like the NH_2 derivatives are better than the corresponding NO_2 counterpart. The difference between SAR in the two assays may due to the membrane permeability of the compounds.

Table 2. Activity of the title compounds against wt HIV-1 RT polymerization.

No.	IC_{50} (μM)[a]
5a3	0.28 ± 0.01
5b2	0.65 ± 0.19
6a1	0.17 ± 0.05
6a2	0.09 ± 0.03
6a3	0.05 ± 0.02
6a4	0.91 ± 0.54
6a5	145.90 ± 93.15
6a6	0.31 ± 0
6a7	0.26 ± 0.05
6a8	0.16 ± 0.004

6a9	0.17 ± 0.01
NVP	2.32 ± 0.59
EFV	0.04 ± 0.01
ETR	0.01 ± 0.00[b]

[a]IC_{50}: Inhibitory concentration of tested compounds required to inhibit biotin deoxyuridine triphosphate (biotin-dUTP) incorporation into the HIV-1 RT by 50%. The data were obtained from Rega institute for medical research, KU Leuven, Belgium.

[b] The data were obtained from the same laboratory of Prof. Erik De Clercq [28].

2.4. Molecular modeling analysis

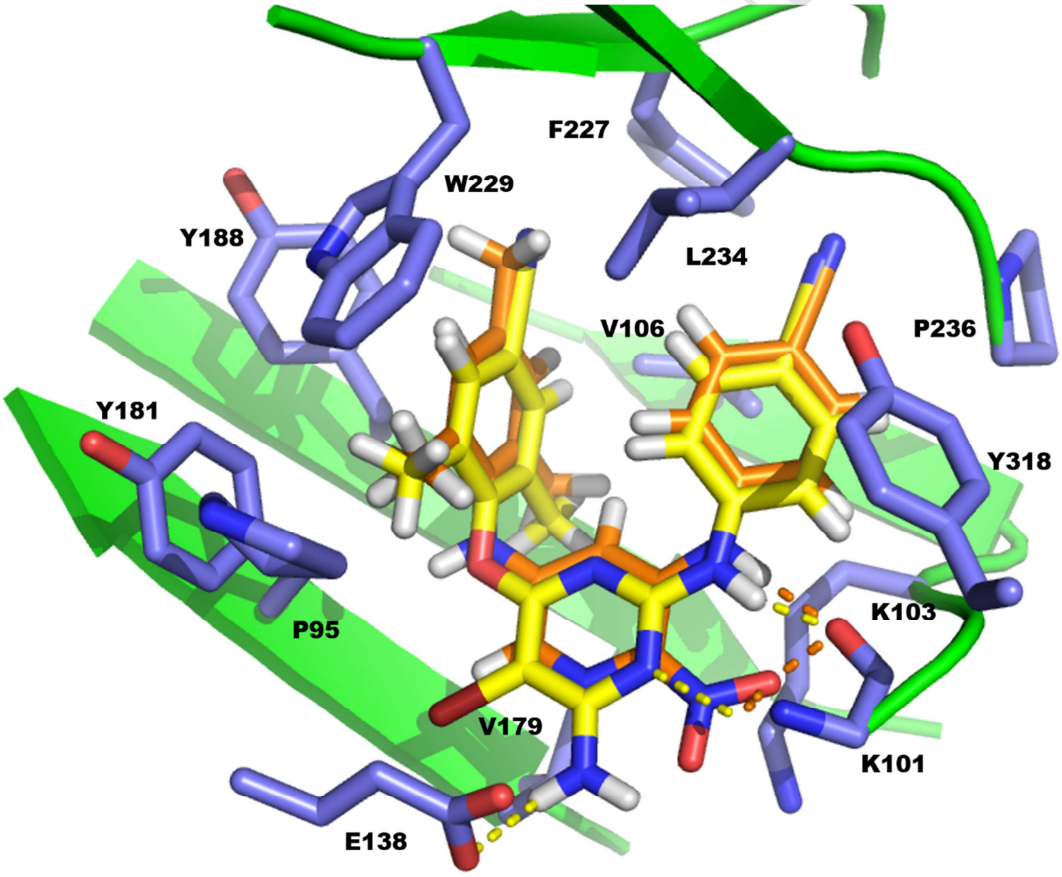

(a)

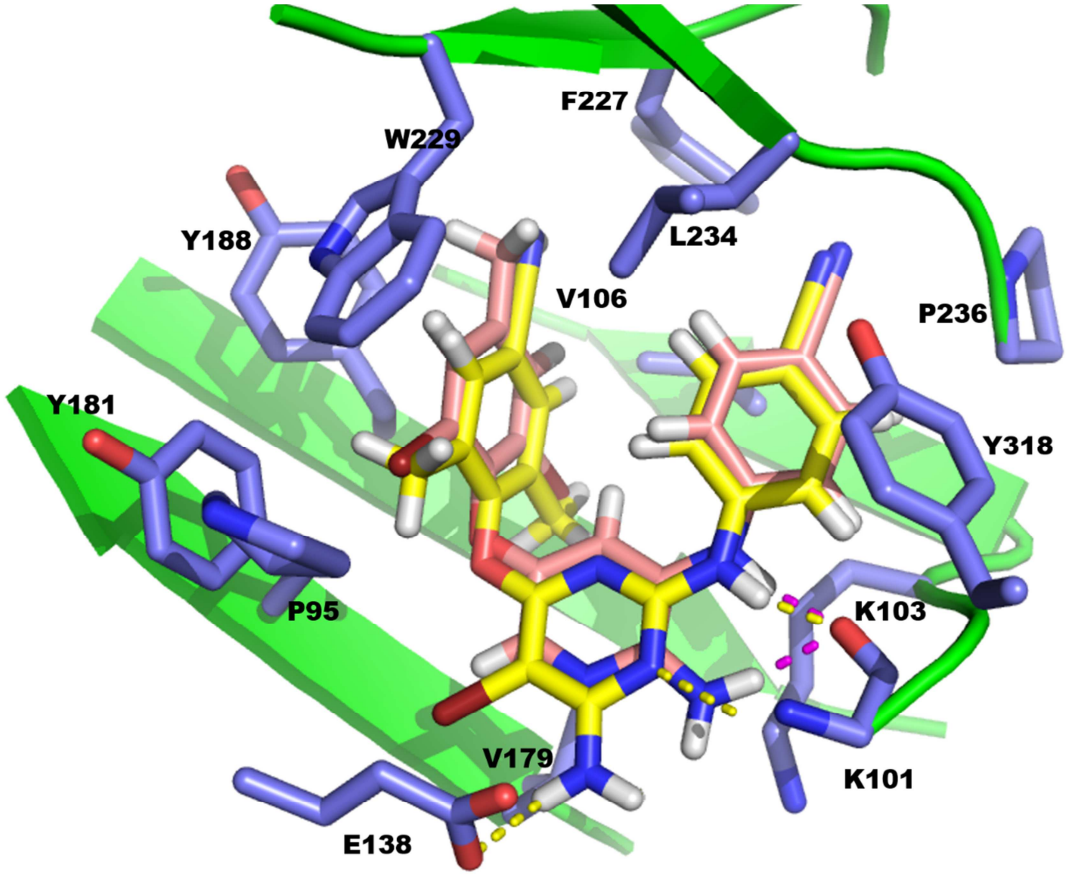

(b)

Figure 2. (a) Predicted binding mode of compound **5b2** (orange) in the allosteric site of HIV-1 wt RT (PDB code: 3MEC) in comparison with the original ligand of this crystal structure ETR (yellow); (b) Predicted binding mode of compound **6a3** (pink) in the allosteric site of HIV-1 wt RT (PDB code: 3MEC) with the comparison with the original ligand of this crystal structure ETR (yellow). The docking results are shown by PyMOL.H-bonding interactions are indicated by dashed lines.

To better understand the structure-affinity relationship for this series of derivatives, the best compound in cell-based HIV-1 infection assay **5b2** and the most potent one in HIV-1 RT inhibition assay **6a3** was docked into the NNRTIs binding pocket (NNIBP, PDB code: 3MEC) using the Surflex-Dock of SYBYL-X 2.0. Default parameters were used as described in the Sybyl-2.0 manual unless otherwise specified, and the result was displayed by PyMOL. The proposed binding modes of these compounds to the NNIBP are shown in **Fig. 2**.

The results indicated a similar binding mode between **5b2**, **6a3** and the original ligand ETR with NNIBP in reverse transcriptase: 1) The left substituted aniline of **5b2** or phenoxy ring of **6a3** all fitted in the hydrophobic cavity surrounded by P95, Y181, Y188, F227 and W229, especially

having a π-π stacking with residue Y188 of RT. Furthermore, the imperfect adaption of the relative bulky OCH_3 of **5a5** and **6a5** as R_2 into the space limited pocket displaced by the modeling may be the reason why OCH_3 led to a decrease in the potency. 2) The right 4-cyanoaniline was located in another pocket and interacted with residues V106, L234, P236 and Y318. 3) The NH connecting the right aniline and the central ring has a strong H-bond with the key residue K101 of RT. Further analysis showed the differences of the polar interactions between the central rings of **5b2** and **6a3** and K101 of RT. The O atom of the nitro group of **5b2** formed a H-bond with the NH_2 on the main chain of K101 and it also had a polar interaction with the C=O of K101. With respect to **6a3**, the NH_2 can also form a H-bond with K101. Since these two groups are out of the pyridine ring, they are closer to K101 than the N atom of pyrimidine of ETR, which may lead to enhanced polar interactions with the binding pocket. However, a H-bond between E138 and ETR was missing from **5b2** or **6a3** causing the observed decreased in potency.

4. Conclusion

In summary, a series of novel diarylpyridine derivatives as novel NNRTIs have been synthesized and evaluated for their bioactivities against HIV-1 (IIIB strain and K103N+Y181C double-mutated strains) and HIV-2 (ROD) in MT-4 cells, as well as against HIV-1 RT activity. These compounds have been designed by a structure-based bioisosterism strategy. Screening results indicated that some compounds showed excellent activity against wt HIV-1 at submicromolar concentrations ranging from 40 nM to 4.41 μM. Taking full advantage of the valuable information from SARs analysis, further optimization of this series of compounds are ongoing in our lab and will be reported in due course.

5. Experimental section

5.1. Chemistry

All melting points were determined on a micromelting point apparatus and are uncorrected. ^{1}H-NMR and ^{13}C-NMR spectra were recorded on a Bruker AV-400 spectrometer using DMSO-d_6 as solvent and tetramethylsilane (TMS) as internal standard. Chemical shifts are reported in parts per million (δ), and signals are expressed as s (singlet), d (doublet), t (triplet), q (quartet) or m (multiplet). Mass spectra were taken on a LC Autosampler Device: Standard G1313A instrument.

TLC was performed on Silica Gel GF254 for TLC (Merck) and spots were visualized by iodine vapors or by irradiation with UV light (254 nm). Flash column chromatography was performed on column packed with Silica Gel 60 (200-300 mesh). Solvents were reagent grade and, when necessary, were purified and dried by standard methods. Concentration of the reaction solutions involved the use of rotary evaporator at reduced pressure.

*5.1.1. Propyl (5-bromopyridin-3-yl)carbamate (**1**)*

To a mixture of 3-amino-5-bromopyridine (5.0 g, 28.9 mmol) and $NaHCO_3$ (7.3 g, 86.9 mmol) in THF (20 mL), propyl chlorocarbonate (9.3 mL, 86.9 mmol) was added dropwise at 0 °C. After stirring for 30 min, THF was removed under reduced pressure. Water (30 mL) was added and extracted with ethyl acetate (3 × 10 mL). The combined organic phase was dried over anhydrous Na_2SO_4 and filtered. The solvent was removed under reduced pressure and the crude propyl (5-bromopyridin-3-yl)carbamate (**1**) was obtained and used in the next step without further purification.

*5.1.2. Propyl (5-bromo-2-nitropyridin-3-yl)carbamate (**2**)*

To a mixture of concentrated H_2SO_4 (15 mL) and propyl (5-bromopyridin-3-yl)carbamate (**1**), fuming HNO_3 (5 mL) was added dropwise at 0 °C. After stirring at 0 °C for 15 min, the mixture was stirred at rt overnight. The mixture was poured into iced water, basified with KOH to pH > 8 and extracted with ethyl acetate (3 × 10 mL). The combined organic phase was dried over anhydrous Na_2SO_4, filtered and concentrated in vacuum. The residue was purified by silica gel column chromatography using ethyl acetate-petroleum ether. Pure fractions were collected and concentrated, giving the desired compound **2** as a yellow solid. Total yield of the above two steps: 80.8%, mp: 74-76°C. ^{1}H NMR (400 MHz, DMSO-*d*6, ppm) δ: 10.11 (s, 1H), 8.48-8.46 (m, 2H), 4.08 (t, 2H, J = 6.7 Hz, OCH_2), 1.64 (sext, 2H, J = 7.3 Hz, CH_2), 0.93 (t, 3H, J = 7.4 Hz, CH_3). ^{13}C-NMR (100 MHz, DMSO-*d*6, ppm) δ: 153.76, 148.01, 143.82, 136.15, 129.79, 124.92, 67.64, 22.15, 10.56.

*5.1.3. 5-Bromo-2-nitropyridin-3-amine (**3**)*

To the reaction mixture of intermediate **2** (0.55g, 9.8 mmol) in 1.5 mL EtOH, KOH (0.55 g, 9.8 mmol) in 8 mL H_2O was added. After stirring at 90 °C for 1 h, the mixture was stirred at rt for

another 1 h. Water (20 mL) was added, and the precipitate was collected by filtration and dried under reduced pressure to give 5-bromo-2-nitropyridin-3-amine (**3**) as a yellow solid. Yield: 94.1%, mp: 183-185 °C. ^{1}H NMR (400 MHz, DMSO-*d*6, ppm) δ: 7.84 (d, J = 2.0 Hz, 1H, pyridine-H), 7.77 (d, 1H, J = 2.0 Hz, pyridine-H), 7.45 (s, 2H, NH_2). ^{13}C-NMR (100 MHz, DMSO-*d*6, ppm) δ: 142.53, 138.93, 136.06, 130.27, 126.43.

*5.1.4. 4-((5-Bromo-2-nitropyridin-3-yl)amino)benzonitrile (**4**)*

Palladium acetate (0.1541 g, 0.69 mmol) and Xantphos (0.3977 g, 0.69mmol) were dissolved in 15 mL dioxane and stirred at ambient temperature for 15 min. 4-Aminobenzonitrile (3.3 g, 14.4 mmol), intermediate **3** (3.0 g, 13.8 mmol) and Cs_2CO_3 (6.7 g, 20.6 mmol) were added. Then the reaction flask was evacuated and backfilled with nitrogen for three times, the resulting mixture was stirred at 100 °C for 12 h. The mixture was filtrated, and the filtrate was collected and concentrated. The crude residue was purified by silica gel column chromatography to provide the title product **4** as a yellow solid. Yield: 78.6%, mp: 241-244 °C. ^{1}H NMR (400 MHz, DMSO-*d*6, ppm) δ: 9.43 (s, 1H, NH), 8.27 (d, J = 1.9 Hz, pyridine-H), 8.19 (d, J = 2.0 Hz, pyridine-H), 7.80 (d, J = 8.7 Hz, Ph-H), 7.41 (d, J = 8.7 Hz, Ph-H). ^{13}C-NMR (100 MHz, DMSO-*d*6, ppm) δ: 145.33, 144.95, 140.96, 135.15, 134.27 (2 × C), 132.30, 126.21, 120.77 (2 × C), 119.54, 105.37. ESI$^-$-MS: *m/z* 317.2 (M-1), 319.2 (M+1). $C_{12}H_7BrN_4O_2$ (317.98).

*5.1.5. General procedure for the synthesis of **5a1-10**.*

To a solution of different substituted phenols (1.03 mmol), 2-picolinic acid (0.0231 g, 0.19 mmol), CuI (0.0179 g, 0.094mmol) and K_3PO_4 (0.4 g, 1.9 mmol) in DMSO (2 mL), intermediate **4** (0.3 g, 0.94 mmol) were added. The reaction flask was evacuated and backfilled with nitrogen for three times, and the resulting mixture was stirred at 90 °C for 24 h. Water (20 mL) was added, the precipitate was collected by filtration and dried under reduced pressure. The precipitate was purified by silica gel column chromatography to provide the title products **5a1-10**.

*5.1.5.1. 4-((5-((4-cyanophenyl)amino)-6-nitropyridin-3-yl)oxy)-3,5-dimethylbenzonitrile (**5a1**)*

Yellow solid, yield: 40.1%, mp: 238-240 °C. ^{1}H NMR (400 MHz, DMSO-*d*6, ppm) δ: 9.45 (s, 1H, NH), 7.84 (d, 1H, J = 2.5 Hz, pyridine-H), 7.75 (s, 2H, Ph-H), 7.73 (d, 2H, J = 8.8 Hz, Ph-H),

7.30 (d, 2H, *J* = 8.7 Hz, Ph-H), 7.01 (d, 1H, *J* = 2.5 Hz, pyridine-H), 2.15 (s, 6H, 2 × CH_3). ^{13}C-NMR (100 MHz, DMSO-*d*6, ppm) *δ*: 157.28, 153.43, 144.90, 141.11, 136.67, 134.05 (2 × C), 133.87 (2 × C), 132.95 (2 × C), 129.01, 120.83 (2 × C), 119.43, 118.74, 112.85, 109.61, 105.32, 15.96 (2 × C). ESI$^+$-MS: *m/z* 386.5 (M+1), 403.6 (M+18), 408.5 (M+23). $C_{21}H_{15}N_5O_3$ (385.12).

*5.1.5.2. 4-((5-(mesityloxy)-2-nitropyridin-3-yl)amino)benzonitrile (**5a2**)*

Yellow solid, yield: 51.2%, mp: 191-193 °C. ^{1}H NMR (400 MHz, DMSO-*d*6, ppm) *δ*: 9.45 (s, 1H, NH), 7.85 (d, 1H, *J* = 2.4 Hz, pyridine-H), 7.72 (d, 2H, *J* = 8.7 Hz, Ph-H), 7.29 (d, 2H, *J* = 8.7 Hz, Ph-H), 6.98 (s, 2H, Ph-H), 6.89 (d, 1H, *J* = 2.5 Hz, pyridine-H), 2.24 (s, 3H, CH_3), 2.06 (s, 6H, 2 × CH_3). ^{13}C-NMR (100 MHz, DMSO-*d*6, ppm) *δ*: 158.51, 147.57, 144.87, 140.58, 136.78, 135.90, 134.01 (2 × C), 130.33 (2 × C), 130.10 (2 × C), 129.37, 120.89 (2 × C), 119.40, 111.95, 105.27, 20.75, 16.03 (2 × C). ESI$^+$-MS: *m/z* 375.4 (M+1), 397.5 (M+23). $C_{21}H_{18}N_4O_3$ (374.14).

*5.1.5.3. 4-((5-(2,6-dibromo-4-methylphenoxy)-2-nitropyridin-3-yl)amino)benzonitrile (**5a3**)*

Yellow solid, yield: 44.3%, mp: 200-203 °C. ^{1}H NMR (400 MHz, DMSO-*d*6, ppm) *δ*: 9.47 (s, 1H, NH), 7.93 (d, 1H, *J* = 2.5 Hz, pyridine-H), 7.74 (d, 2H, *J* = 8.7 Hz, Ph-H), 7.68 (s, 2H, Ph-H), 7.28 (d, 2H, *J* = 8.8 Hz, Ph-H), 7.08 (d, 1H, *J* = 2.5 Hz, pyridine-H), 2.33 (s, 3H, CH_3). ^{13}C-NMR (100 MHz, DMSO-*d*6, ppm) *δ*: 156.87, 144.90, 144.87, 141.49, 140.59, 136.21, 134.31 (2 × C), 134.12 (2 × C), 129.32, 120.59 (2 × C), 119.42, 116.94, 113.46, 105.31, 20.22. ESI$^-$-MS: *m/z* 503.2 (M+1), 505.2 (M+3). $C_{19}H_{12}Br_2N_4O_3$ (501.93).

*5.1.5.4. 4-((5-(2,6-dimethylphenoxy)-2-nitropyridin-3-yl)amino)benzonitrile (**5a4**)*

Yellow solid, yield: 47.3%, mp: 190-192 °C. ^{1}H NMR (400 MHz, DMSO-*d*6, ppm) *δ*: 9.45 (s, 1H, NH), 7.88 (d, 1H, *J* = 2.4 Hz, pyridine-H), 7.71 (d, 2H, *J* = 8.7 Hz, Ph-H), 7.29 (d, 2H, *J* = 8.8 Hz, Ph-H), 7.20-7.12 (m, 3H, Ph-H), 6.87 (d, 1H, *J* = 2.5 Hz, pyridine-H), 2.10 (s, 6H, 2 × CH_3). ^{13}C-NMR (100 MHz, DMSO-*d*6, ppm) *δ*: 158.29, 149.69, 144.78, 140.54, 136.84, 133.99 (2 × C), 130.55 (2 × C), 129.91 (2 × C), 129.37, 126.88, 120.95 (2 × C), 119.40, 111.73, 105.33, 16.10 (2 × C). ESI$^+$-MS: *m/z* 361.4 (M+1), 383.4 (M+23). $C_{20}H_{16}N_4O_3$ (360.12).

*5.1.5.5. 4-((5-(2,6-dimethoxyphenoxy)-2-nitropyridin-3-yl)amino)benzonitrile (**5a5**)*

Yellow solid, yield: 43.4%, mp: 218-222 °C. ^{1}H NMR (400 MHz, DMSO-*d*6, ppm) *δ*: 9.42 (s,

1H, NH), 7.92 (d, 1H, *J* = 2.5 Hz, pyridine-H), 7.75 (d, 2H, *J* = 8.7 Hz, Ph-H), 7.26 (d, 2H, *J* = 8.8 Hz, Ph-H), 7.25 (t, 1H, *J* = 8.5 Hz, Ph-H), 6.93 (d, 1H, *J* = 2.5 Hz, pyridine-H), 6.82 (d, 2H, *J* = 8.5 Hz, Ph-H), 3.78 (s, 6H, 2 × CH_3). ^{13}C-NMR (100 MHz, DMSO-*d*6, ppm) *δ*: 158.65, 152.58 (2 × C), 144.92, 140.57, 136.34, 134.07 (2 × C), 129.72, 127.61, 120.52 (2 × C), 119.43, 111.95, 105.94 (2 × C), 105.16, 56.59 (2 × C). ESI$^-$-MS: *m/z* 391.5 (M-1). $C_{20}H_{16}N_4O_5$ (392.11).

*5.1.5.6. 4-((5-(4-chloro-2,6-dimethylphenoxy)-2-nitropyridin-3-yl)amino)benzonitrile (**5a6**)*

Yellow solid, yield: 44.4%, mp: 230-233 °C. ^{1}H NMR (400 MHz, DMSO-*d*6, ppm) *δ*: 9.45 (s, 1H, NH), 7.86 (d, 1H, *J* = 2.4 Hz, pyridine-H), 7.73 (d, 2H, *J* = 8.7 Hz, Ph-H), 7.30 (d, 2H, *J* = 8.6 Hz, Ph-H), 7.30 (s, 2H, Ph-H), 6.95 (d, 1H, *J* = 2.5 Hz, pyridine-H), 2.10 (s, 6H, 2 × CH_3). ^{13}C-NMR (100 MHz, DMSO-*d*6, ppm) *δ*: 157.88, 148.62, 140.90, 140.86, 136.72, 134.03 (2 × C), 133.10 (2 × C), 130.54, 129.37 (2 × C), 129.18, 120.88 (2 × C), 119.42, 112.39, 105.30, 16.00 (2 × C). ESI$^+$-MS: *m/z* 395.3 (M+1), 397.4 (M+3), 417.5 (M+23). $C_{20}H_{15}ClN_4O_3$ (394.08).

*5.1.5.7. 4-((5-(4-bromo-2,6-dimethylphenoxy)-2-nitropyridin-3-yl)amino)benzonitrile (**5a7**)*

Yellow solid, yield: 47.2%, mp: 237-240 °C. ^{1}H NMR (400 MHz, DMSO-*d*6, ppm) *δ*: 9.45 (s, 1H, NH), 7.86 (d, 1H, *J* = 2.4 Hz, pyridine-H), 7.73 (d, 2H, *J* = 8.7 Hz, Ph-H), 7.43 (s, 2H, Ph-H), 7.30 (d, 2H, *J* = 8.7 Hz, Ph-H), 6.95 (d, 1H, *J* = 2.4 Hz, pyridine-H), 2.10 (s, 6H, 2 × CH_3). ^{13}C-NMR (100 MHz, DMSO-*d*6, ppm) *δ*:157.80, 149.13, 144.90, 140.85, 136.71, 134.02 (2 × C), 133.47 (2 × C), 132.20 (2 × C), 129.18, 120.88 (2 × C), 119.42, 118.92, 112.42, 105.31, 15.90 (2 × C). ESI$^-$-MS: *m/z* 437.4 (M-1). $C_{20}H_{15}BrN_4O_3$ (438.03).

*5.1.5.8. 4-((2-nitro-5-(2,4,6-trichlorophenoxy)pyridin-3-yl)amino)benzonitrile (**5a8**)*

Yellow solid, yield: 54.9%, mp: 213-216 °C. ^{1}H NMR (400 MHz, DMSO-*d*6, ppm) *δ*: 9.47 (s, 1H, NH), 7.97 (d, 1H, *J* = 2.5 Hz, pyridine-H), 7.93 (s, 2H, Ph-H), 7.76 (d, 2H, *J* = 8.8 Hz, Ph-H), 7.33-7.30 (m, 3H).^{13}C-NMR (100 MHz, DMSO-*d*6, ppm) *δ*: 156.52, 145.03, 144.50, 141.92, 136.17, 134.11 (2 × C), 132.35, 130.23 (2 × C), 129.40, 128.96, 120.48 (2 × C), 119.46, 114.15, 105.23. ESI$^-$-MS: *m/z* 433.4 (M-1), 435.3 (M+1), 437.3 (M+3). $C_{18}H_9Cl_3N_4O_3$ (433.97).

*5.1.5.9. 4-((2-nitro-5-(2,4,6-tribromophenoxy)pyridin-3-yl)amino)benzonitrile (**5a9**)*

Yellow solid, yield: 44.9%, mp: 235-240 °C. ^{1}H NMR (400 MHz, DMSO-*d*6, ppm) *δ*: 9.47 (s,

1H, NH), 8.14 (s, 2H, Ph-H), 7.96 (d, 1H, *J* = 2.5 Hz, pyridine-H), 7.75 (d, 2H, *J* = 8.7 Hz, Ph-H), 7.29 (d, 2H, *J* = 8.8 Hz, Ph-H), 7.23 (d, 1H, *J* = 2.5 Hz, pyridine-H). ^{13}C-NMR (100 MHz, DMSO-*d*6, ppm) *δ*: 156.37, 147.01, 145.02, 141.81, 136.15, 136.09, 134.13 (2 × C), 129.31, 120.88, 120.43 (2 × C), 119.45, 118.68, 114.16, 105.22. ESI$^-$-MS: *m/z* 565.2 (M-1), 567.2 (M+1), 571.2 (M+5). $C_{18}H_9Br_3N_4O_3$ (565.82).

*5.1.5.10. 4-((2-nitro-5-(2,4,6-trifluorophenoxy)pyridin-3-yl)amino)benzonitrile (**5a10**)*

Yellow solid, yield: 44.0%, mp: 218-221 °C. ^{1}H NMR (400 MHz, DMSO-*d*6, ppm) *δ*: 9.48 (s, 1H, NH), 8.04 (d, 1H, *J* = 2.5 Hz, pyridine-H), 7.77 (d, 2H, *J* = 8.7 Hz, Ph-H), 7.56-7.51 (m, 2H, Ph-H), 7.45 (d, 1H, *J* = 2.5 Hz, pyridine-H), 7.34 (d, 2H, *J* = 8.7 Hz, Ph-H). ^{13}C-NMR (100 MHz, DMSO-*d*6, ppm) *δ*: 159.40 (dt, J_1 = 238.5 Hz, J_2 = 14.6 Hz), 157.32, 155.33 (ddd, J_1 = 248.8 Hz, J_2 = 15.9 Hz, J_3 = 6.3 Hz), 144.98, 141.86, 136.25, 134.11 (2 × C), 128.87, 126.60 (td, J_1 = 15.0 Hz, J_2 = 5.5 Hz), 120.62 (2 × C), 119.47, 114.15, 105.31, 102.93 (t, *J* = 27.3 Hz,). ESI$^-$-MS: *m/z* 385.3 (M-1). $C_{18}H_9F_3N_4O_3$ (386.06).

*5.1.6. General procedure for the synthesis of **5b1** and **5b2**.*

Palladium acetate (0.0176 g, 0.079 mmol) and Xantphos (0.0453 g, 0.079mmol) were dissolved in 20 mL dioxane and stirred at ambient temperature for 15 min. Intermediate **4** (0.50 g, 1.57 mmol), substituted aniline (1.73 mmol) and Cs_2CO_3 (0.77 g, 236 mmol) were added. Then the reaction flask was evacuated and backfilled with nitrogen for three times, the resulting mixture was stirred at 100 °C for 12 h. The reaction mixture was filtrated, and the filtrate was collected and concentrated. The crude residue was purified by silica gel column chromatography to provide the title product **5b1-2**.

*5.1.6.1. 4-((5-((2,6-dimethylphenyl)amino)-2-nitropyridin-3-yl)amino)benzonitrile (**5b1**)*

Yellow solid, yield: 76.4%, mp: 251-254 °C. ^{1}H NMR (400 MHz, DMSO-*d*6, ppm) *δ*: 9.44 (s, 1H, NH), 8.87 (s, br, 1H), 7.72 (d, 2H, *J* = 8.1 Hz, Ph-H), 7.53 (s, br, 1H), 7.32 (d, 2H, *J* = 6.8 Hz, Ph-H), 7.18-7.11 (m, 3H, Ph-H), 6.31 (s, br, 1H), 2.15 (s, 6H, 2 × CH_3). ^{13}C-NMR (100 MHz, DMSO-*d*6, ppm) *δ*: 149.11, 144.84, 137.89, 136.68, 136.14 (2 × C), 135.71, 133.94 (2 × C), 129.07 (2 × C), 127.66, 121.40 (2 × C), 119.46, 105.05, 18.19 (2 × C). ESI$^+$-MS: *m/z* 360.5 (M+1) 382.8 (M+23). $C_{20}H_{17}N_5O_2$ (359.14).

*5.1.6.2. 4-((5-(mesitylamino)-2-nitropyridin-3-yl)amino)benzonitrile (**5b2**)*

Yellow solid, yield: 67.2%, mp: 217-222 °C. ^{1}H NMR (400 MHz, DMSO-*d*6, ppm) *δ*: 9.42 (s, 1H, NH), 8.78 (s, br, 1H), 7.73 (d, 2H, *J* = 5.9 Hz), 7.31-7.23 (m, 3H), 6.96 (s, 2H, Ph-H), 6.07 (s, br, 1H), 2.23 (s, 3H, CH_3), 2.10 (s, 6H, 2 × CH_3). ^{13}C-NMR (100 MHz, DMSO-*d*6, ppm) *δ*:149.37, 144.95, 137.84, 136.77, 136.68, 135.85 (2 × C), 133.96 (2 × C), 133.07, 129.65 (2 × C), 121.30, 119.47, 104.96, 20.96, 18.10 (2 × C).ESI^{+}-MS: *m/z* 374.5 (M+1), 396.4 (M+23). $C_{21}H_{19}N_5O_2$ (373.15).

*5.1.7. General procedure for the synthesis of **6a1-9**.*

To a solution of derivatives **5a1-9** (0.45 mmol) in EtOH (5 mL), $SnCl_2.2H_2O$ (2.25 mmol) was added. The reaction flask was evacuated and backfilled with nitrogen for three times, the reaction mixture was stirred at reflux overnight. After removal of the solvent under reduced pressure, water (15 mL) was added. The mixture was alkalized with K_2CO_3 to pH >8 and extracted with ethyl acetate (3×10 mL). The combined organic phase was dried over anhydrous Na_2SO_4, filtered and concentrated in vacuum. Recrystallization from ethyl acetate afforded the title products **6a1-9**.

*5.1.7.1. 4-((6-amino-5-((4-cyanophenyl)amino)pyridin-3-yl)oxy)-3,5-dimethylbenzonitrile (**6a1**)*

White solid, yield: 70.0%, mp: 238-240 °C. ^{1}H NMR (400 MHz, DMSO-*d*6, ppm) *δ*: 8.16 (s, 1H, NH), 7.67 (s, 2H, Ph-H), 7.56 (d, 2H, *J* = 8.7 Hz, Ph-H), 7.40 (d, 1H, *J* = 2.7 Hz, pyridine-H), 6.91 (d, 1H, *J* = 2.7 Hz, pyridine-H), 6.76 (d, 2H, *J* = 8.8 Hz, Ph-H), 5.56 (s, 2H, NH_2), 2.15 (s, 6H, 2 × CH_3). ^{13}C-NMR (100 MHz, DMSO-*d*6, ppm) *δ*: 155.47, 150.96, 149.33, 145.72, 133.97 (2 × C), 133.62 (2 × C), 133.19 (2 × C), 130.46, 121.61, 120.42, 119.07, 119.03, 114.82 (2 × C), 108.27, 99.52, 16.29 (2 × C). ESI^{+}-MS: *m/z* 356.5 (M+1). $C_{21}H_{17}N_5O$ (355.14).

*5.1.7.2. 4-((2-amino-5-(mesityloxy)pyridin-3-yl)amino)benzonitrile (**6a2**)*

Light yellow solid, yield: 64.2%, mp: 210-212 °C. ^{1}H NMR (400 MHz, DMSO-*d*6, ppm) *δ*: 8.15 (s, 1H, NH), 7.55 (d, 2H, *J* = 8.8 Hz, Ph-H), 7.42 (d, 1H, *J* = 2.7 Hz, pyridine-H), 6.92 (s, 2H, Ph-H), 6.78 (d, 1H, *J* = 2.7 Hz, pyridine-H), 6.74 (d, 2H, *J* = 8.8 Hz, Ph-H), 5.44 (s, 2H, NH_2), 2.23 (s, 3H, CH_3), 2.06 (s, 6H, 2 × CH_3). ^{13}C-NMR (100 MHz, DMSO-*d*6, ppm) *δ*: 150.40, 149.49,

149.15, 146.65, 134.49, 133.96 (2 × C), 130.61, 130.55, 130.08 (2 × C), 121.38, 120.44, 118.68, 114.68 (2 × C), 99.34, 20.79, 16.37 (2 × C). ESI^+-MS: *m/z* 345.4 (M+1). $C_{21}H_{20}N_4O$ (344.16).

*5.1.7.3. 4-((2-amino-5-(2,6-dibromo-4-methylphenoxy)pyridin-3-yl)amino)benzonitrile (**6a3**)*

White solid, yield: 66.5%, mp: 229-230 °C. ^{1}H NMR (400 MHz, DMSO-*d*6, ppm) *δ*: 8.17 (s, 1H, NH), 7.61 (s, 2H, Ph-H), 7.56 (d, 2H, *J* = 8.7 Hz, Ph-H), 7.46 (d, 1H, *J* = 2.7 Hz, pyridine-H), 6.86 (d, 1H, *J* = 2.7 Hz, pyridine-H), 6.77 (d, 2H, *J* = 8.8 Hz, Ph-H), 5.58 (s, 2H, NH_2), 2.31 (s, 6H, 2 × CH_3). ^{13}C-NMR (100 MHz, DMSO-*d*6, ppm) *δ*: 151.08, 149.37, 146.65, 145.43, 139.20, 134.10 (2 × C), 133.99 (2 × C), 130.92, 121.25, 120.41, 119.09, 117.77, 114.75 (2 × C), 99.51, 20.16. ESI^+-MS: *m/z* 475.1 (M+1). $C_{19}H_{14}Br_2N_4O$ (471.95).

*5.1.7.4. 4-((2-amino-5-(2,6-dimethylphenoxy)pyridin-3-yl)amino)benzonitrile (**6a4**)*

White solid, yield: 65.5%, mp: 224-226 °C. ^{1}H NMR (400 MHz, DMSO-*d*6, ppm) *δ*: 8.15 (s, 1H, NH), 7.55 (d, 2H, *J* = 8.6 Hz, Ph-H), 7.42 (d, 1H, *J* = 2.6 Hz, pyridine-H), 7.14-7.04 (m, 3H), 6.80 (d, 1H, *J* = 2.5 Hz, pyridine-H), 6.74 (d, 2H, *J* = 8.7 Hz, Ph-H), 5.46 (s, 2H, NH_2), 2.11 (s, 6H, 2 × CH_3). ^{13}C-NMR (100 MHz, DMSO-*d*6, ppm) *δ*: 151.38, 150.42, 149.41, 146.48, 1333.96 (2 × C), 131.05, 130.46, 129.61 (2 × C), 125.64, 121.44, 120.43, 118.58, 114.72 (2 × C), 99.39, 16.45 (2 × C). ESI^+-MS: *m/z* 331.5 (M+1). $C_{20}H_{18}N_4O$ (330.15).

*5.1.7.5. 4-((2-amino-5-(2,6-dimethoxyphenoxy)pyridin-3-yl)amino)benzonitrile (**6a5**)*

White solid, yield: 68.9%, mp: 205-207 °C. ^{1}H NMR (400 MHz, DMSO-*d*6, ppm) *δ*: 8.13 (s, 1H, NH), 7.56 (d, 2H, *J* = 8.7 Hz, Ph-H), 7.51 (d, 1H, *J* = 2.7 Hz, pyridine-H), 7.15 (t, 1H, *J* = 8.4 Hz, Ph-H), 6.79 (d, 1H, *J* = 2.7 Hz, pyridine-H), 6.80-6.73 (m, 4H), 5.42 (s, br, 2H, NH_2), 3.74 (s, 6H, 2 × CH_3). ^{13}C-NMR (100 MHz, DMSO-*d*6, ppm) *δ*: 153.46, 150.24, 149.54, 147.29, 133.96 (2 × C), 132.27, 131.12, 126.12, 120.87, 120.46, 119.00, 114.52 (2 × C), 106.02 (2 × C), 99.26, 56.43 (2 × C). ESI^+-MS: *m/z* 363.4 (M+1). $C_{20}H_{18}N_4O_3$ (362.14).

*5.1.7.6. 4-((2-amino-5-(4-chloro-2,6-dimethylphenoxy)pyridin-3-yl)amino)benzonitrile (**6a6**)*

Light yellow solid, yield: 76.4%, mp: 227-231 °C. ^{1}H NMR (400 MHz, DMSO-*d*6, ppm) *δ*: 8.16 (s, 1H, NH), 7.56 (d, 2H, *J* = 8.6 Hz, Ph-H), 7.42 (d, 1H, *J* = 2.4 Hz, pyridine-H), 7.23 (s, 2H, Ph-H), 6.86 (d, 1H, *J* = 2.4 Hz, pyridine-H), 6.76 (d, 2H, *J* = 8.6 Hz, Ph-H), 5.50 (s, 2H, NH_2),

2.11 (s, 6H, 2 × CH_3). ^{13}C-NMR (100 MHz, DMSO-*d*6, ppm) *δ*:150.66, 150.33, 149.38, 146.14, 133.96 (2 × C), 133.49 (2 × C), 130.36, 129.22, 129.06 (2 × C), 121.52, 120.43, 118.74, 114.77 (2 × C), 99.45, 16.31 (2 × C). ESI$^+$-MS: *m/z* 365.4 (M+1), 367.3 (M+3). $C_{20}H_{17}ClN_4O$ (364.11).

*5.1.7.7. 4-((2-amino-5-(4-bromo-2,6-dimethylphenoxy)pyridin-3-yl)amino)benzonitrile (**6a7**)*

Light yellow solid, yield: 64.4%, mp: 222-225 °C. ^{1}H NMR (400 MHz, DMSO-*d*6, ppm) *δ*: 8.16 (s, 1H, NH), 7.56 (d, 2H, *J* = 8.7 Hz, Ph-H), 7.41 (d, 1H, *J* = 2.7 Hz, pyridine-H), 7.36 (s, 2H, Ph-H), 6.85 (d, 1H, *J* = 2.7 Hz, pyridine-H), 6.75 (d, 2H, *J* = 8.8 Hz, Ph-H), 5.50 (s, 2H, NH_2), 2.10 (s, 6H, 2 × CH_3). ^{13}C-NMR (100 MHz, DMSO-*d*6, ppm) *δ*: 150.85, 150.68, 149.39, 146.07, 133.96 (2 × C), 133.92 (2 × C), 131.99 (2 × C), 130.40, 121.52, 120.43, 118.78, 117.55, 114.78 (2 × C), 99.45, 16.23 (2 × C). ESI$^+$-MS: *m/z* 409.5 (M+1). $C_{20}H_{17}BrN_4O$ (408.06).

*5.1.7.8. 4-((2-amino-5-(2,4,6-trichlorophenoxy)pyridin-3-yl)amino)benzonitrile(**6a8**)*

White solid, yield: 65.4%, mp: 245-250 °C. ^{1}H NMR (400 MHz, DMSO-*d*6, ppm) *δ*: 8.19 (s, 1H, NH), 7.83 (s, 2H, Ph-H), 7.57 (d, 2H, *J* = 8.7 Hz, Ph-H), 7.51 (d, 1H, *J* = 2.8 Hz, pyridine-H), 7.02 (d, 1H, *J* = 2.7 Hz, pyridine-H), .6.78 (d, 2H, *J* = 8.8 Hz, Ph-H), 5.65 (s, 2H, NH_2). ^{13}C-NMR (100 MHz, DMSO-*d*6, ppm) *δ*: 151.52, 149.36, 146.51, 145.35, 133.98 (2 × C), 130.94, 130.80, 129.96, 129.95, 121.37, 120.42, 119.41, 114.78 (2 × C), 99.54. ESI$^+$-MS: *m/z* 405.4 (M+1) 407.4 (M+3) 409.4 (M+5). $C_{18}H_{11}Cl_3N_4O$ (404.00).

*5.1.7.9. 4-((2-amino-5-(2,4,6-tribromophenoxy)pyridin-3-yl)amino)benzonitrile (**6a9**)*

Light yellow solid, yield: 71.3%, mp: 255-258 °C. ^{1}H NMR (400 MHz, DMSO-*d*6, ppm) *δ*: 8.18 (s, 1H, NH), 8.06 (s, 2H, Ph-H), 7.56 (d, 2H, *J* = 8.7 Hz, Ph-H), 7.47 (d, 1H, *J* = 2.6 Hz, pyridine-H), 6.94 (d, 1H, *J* = 2.6 Hz, pyridine-H), .6.78 (d, 2H, *J* = 8.7 Hz, Ph-H), 5.62 (s, 2H, NH_2). ^{13}C-NMR (100 MHz, DMSO-*d*6, ppm) *δ*: 151.30, 149.36, 148.82, 145.06, 135.92 (2 × C), 133.99 (2 × C), 130.87, 121.34, 120.42, 119.40 (2 × C), 119.30, 114.79 (2 × C), 99.52. ESI$^+$-MS: *m/z* 539.2 (M+1) 541.2 (M+3) 543.1 (M+5). $C_{18}H_{11}Br_3N_4O$ (535.85).

5.2. Biological activity

5.2.1. In vitro anti-HIV assay

The methodology of the anti-HIV assay has been previously described [12, 22, 23]. Stock solutions (10 × final concentration) of test compounds were added in 25 µL volumes to two series of triplicate wells to allow simultaneous evaluation of their effects on mock- and HIV-infected cells at the beginning of each experiment. Serial fivefold dilutions of test compounds were made directly in flat-bottomed 96-well microtiter trays using a Biomek 3000 robot (Beckman instruments, Fullerton, CA). Untreated control HIV- and mock-infected cell samples were included for each sample.

HIV-1 [29] (IIIB, RES056) or HIV-2 [30] (ROD) stock (50 µL) at 100-300 $CCID_{50}$ (cell culture infectious dose) or culture medium was added to either the infected or mock-infected wells of the microtiter tray. Mock-infected cells were used to evaluate the effect of test compound on uninfected cells in order to assess the cytotoxicity of the tested compound. Exponentially growing MT-4 cells were centrifuged for 5 min at 220 g and the supernatant was discarded. The MT-4 cells were resuspended at 6×10^5 cells/mL, and 50 µL volumes were transferred to the microtiter tray wells. Five days after infection, the viability of mock- and HIV-infected cells was examined spectrophotometrically by the MTT assay.

The MTT assay is based on the reduction of yellow colored 3-(4,5-dimethylthiazol-2-yl)-2,5-diphenyltetrazolium bromide (MTT) (Acros Organics, Geel, Belgium) by mitochondrial dehydrogenase of metabolically active cells to a blue-purple formazan that can be measured spectrophotometrically. The absorbances were read in a computer-controlled photometer (Infinite M1000, Tecan, Mechelen, Belgium), at two wavelengths (540 and 690 nm). All data were calculated using the median OD (optical density) value of three wells. The 50% cytotoxic concentration (CC_{50}) was defined as the concentration of the test compound that reduced the absorbance (OD540) of the mock-infected control samples by 50%. The 50% effective concentration (EC_{50}) was defined as the compound concentration required for inhibiting virus-induced syncytium formation by 50%.

5.2.2. HIV-1 RT inhibition assay

Recombinant wild type p66/p51 HIV-1 RT was expressed and purified as described. The RT assay is performed with the EnzCheck Reverse Transcriptase Assay kit (Molecular Probes,

Invitrogen), as described by the manufacturer. The assay is based on the dsDNA quantitation reagent PicoGreen. This reagent shows a pronounced increase in fluorescence signal upon binding to dsDNA or RNA-DNA heteroduplexes. Single-stranded nucleic acids generate only minor fluorescence signal enhancement when a sufficiently high dye:base pair ratio is applied. This condition is met in the assay.

A poly(rA) template of approximately 350 bases long, and an oligo$(dT)_{16}$ primer, are annealed in a molar ratio of 1:1.2 (60 min. at room temperature). 52 ng of the RNA/DNA is brought into each well of a 96-well plate in a volume of 20 µL polymerization buffer (60 mM Tris-HCl, 60 mM KCl, 8 mM $MgCl_2$, 13 mM DTT, 100 µM dTTP, pH 8.1). 5 µl of RT enzyme solution, diluted to a suitable concentration in enzyme dilution buffer (50 mM Tris-HCl, 20% glycerol, 2 mM DTT, pH = 7.6), is added. The reactions are incubated at 25°C for 40 minutes and then stopped by the addition of EDTA (15 mM). Heteroduplexes are then detected by addition of PicoGreen. Signals are read using an excitation wavelength of 490 nm and emission detection at 523 nm using a spectrofluorometer (Safire2, Tecan). To test the activity of compounds against RT, 1 µl of compound in DMSO is added to each well before the addition of RT enzyme solution. Control wells without compound contain the same amount of DMSO. Results are expressed as relative fluorescence i.e. the fluorescence signal of the reaction mix with compound divided by the signal of the same reaction mix without compound.

5.3. Molecular modeling

Structures of **5b2** and **6a3** was drawn, optimized and docked into the published three-dimensional crystal structures of wt RT (complexes with ETR, PDB code: 3MEC, retrieved from the Protein Data Bank) by means of surflex-docking module of Sybyl-2.0. Top scoring poses were shown by PyMOL version 1.7.0 (http://www.pymol.org/), in overlap with the bound ligand (ETR) in the binding site of RT. The secondary structure of RT is shown in cartoons, and only the key residues for interactions with the inhibitors were shown in sticks and labeled. The potential hydrogenbonds were presented by dashed lines. More detailed method is described previously [13].

Note

The authors declare no conflict of interest.

Acknowledgment

Financial support from the National Natural Science Foundation of China (NSFC Nos. 81273354), Key Project of NSFC for International Cooperation (Nos. 81420108027), Young Scholars Program of Shandong University (YSPSDU, for P.Z.), and Major Project of Science and Technology of Shandong Province (No. 2015ZDJS04001) and KU Leuven (GOA 10/014) is gratefully acknowledged. We thank K. Erven, K. Uyttersprot and C. Heens for technical assistance with the HIV assays.

Supplementary Material

MS, ^{1}H NMR and ^{13}C NMR of title compounds can be found in the Supplementary Material.

References

[1] D. Li, P. Zhan, E. De Clercq, X. Liu, Strategies for the design of HIV-1 non-nucleoside reverse transcriptase inhibitors: lessons from the development of seven representative paradigms, J. Med. Chem., 55 (2012) 3595-3613.

[2] P. Zhan, X. Liu, Z. Li, C. Pannecouque, E. De Clercq, Design strategies of novel NNRTIs to overcome drug resistance, Curr. Med. Chem., 16 (2009) 3903-3917.

[3] P. Zhan, X. Chen, D. Li, Z. Fang, E. De Clercq, X. Liu, HIV-1 NNRTIs: structural diversity, pharmacophore similarity, and implications for drug design, Med. Res. Rev., 33 Suppl 1 (2013) E1-72.

[4] Y. Song, Z. Fang, P. Zhan, X. Liu, Recent advances in the discovery and development of novel HIV-1 NNRTI platforms (Part II): 2009-2013 update, Curr. Med. Chem., 21 (2014) 329-355.

[5] Z. Xu, J. Guo, Y. Yang, M. Zhang, M. Ba, Z. Li, Y. Cao, R. He, M. Yu, H. Zhou, X. Huang, Y. Guo, C. Guo, 2,4,5-Trisubstituted thiazole derivatives as HIV-1 NNRTIs effective on both wild-type and mutant HIV-1 reverse transcriptase: Optimization of the substitution of positions 4 and 5, Eur. J. Med. Chem., 123 (2016) 309.

[6] R. Schrijvers, Etravirine for the treatment of HIV/AIDS, Expert Opin. Pharmacother., 14 (2013) 1087-1096.

[7] E. Seminari, A. Castagna, A. Lazzarin, Etravirine for the treatment of HIV infection, Expert Rev. Anti Infect. Ther., 6 (2008) 427-433.

[8] M. Schöller-Gyüre, T.N. Kakuda, G. De Smedt, H. Vanaken, M.-P. Bouche, M. Peeters, B. Woodfall, R.M.W. Hoetelmans, A pharmacokinetic study of etravirine (TMC125) co-administered with ranitidine and omeprazole in HIV–negative volunteers, Br. J. Clin. Pharmacol., 66 (2008) 508-516.

[9] E.B. Lansdon, K.M. Brendza, M. Hung, R. Wang, S. Mukund, D. Jin, G. Birkus, N. Kutty, X. Liu, Crystal structures of HIV-1 reverse transcriptase with etravirine (TMC125) and rilpivirine (TMC278): implications for drug design, J. Med. Chem., 53 (2010) 4295-4299.

[10] X. Tian, B. Qin, Z. Wu, X. Wang, H. Lu, S.L. Morris-Natschke, C.H. Chen, S. Jiang, K.H. Lee, L. Xie, Design, synthesis, and evaluation of diarylpyridines and diarylanilines as potent non-nucleoside HIV-1 reverse transcriptase inhibitors, J. Med. Chem., 53 (2010) 8287-8297.

[11] B. Qin, X. Jiang, H. Lu, X. Tian, F. Barbault, L. Huang, K. Qian, C.H. Chen, R. Huang, S. Jiang, K.H. Lee, L. Xie, Diarylaniline derivatives as a distinct class of HIV-1 non-nucleoside reverse transcriptase inhibitors, J. Med. Chem., 53 (2010) 4906-4916.

[12] Y. Tian, D. Du, D. Rai, L. Wang, H. Liu, P. Zhan, E. De Clercq, C. Pannecouque, X. Liu, Fused heterocyclic compounds bearing bridgehead nitrogen as potent HIV-1 NNRTIs. Part 1: design, synthesis and biological evaluation of novel 5,7-disubstituted pyrazolo[1,5-a]pyrimidine derivatives, Bioorg. Med. Chem., 22 (2014) 2052-2059.

[13] L. Wang, Y. Tian, W. Chen, H. Liu, P. Zhan, D. Li, H. Liu, E. De Clercq, C. Pannecouque, X. Liu, Fused heterocycles bearing bridgehead nitrogen as potent HIV-1 NNRTIs. Part 2: discovery of novel [1,2,4]Triazolo[1,5-a]pyrimidines using a structure-guided core-refining approach, Eur. J. Med. Chem., 85 (2014) 293-303.

[14] J. Yang, W. Chen, D. Kang, X. Lu, X. Li, Z. Liu, B. Huang, D. Daelemans, C. Pannecouque, E. De Clercq, P. Zhan, X. Liu, Design, synthesis and anti-HIV evaluation of novel diarylpyridine derivatives targeting the entrance channel of NNRTI binding pocket, Eur. J. Med. Chem., 109 (2016) 294-304.

[15] Q. Meng, X. Chen, D. Kang, B. Huang, W. Li, P. Zhan, D. Daelemans, E. De Clercq, C. Pannecouque, X. Liu, Design, synthesis and evaluation of novel HIV-1 NNRTIs with dual structural conformations targeting the entrance channel of the NNRTI binding pocket, Eur. J. Med. Chem., 115 (2016) 53-62.

[16] W. Chen, P. Zhan, D. Daelemans, J. Yang, B. Huang, E. De Clercq, C. Pannecouque, X. Liu, Structural optimization of pyridine-type DAPY derivatives to exploit the tolerant regions of the NNRTI binding pocket, Eur. J. Med. Chem., 121 (2016) 352-363.

[17] D. Li, P. Zhan, H. Liu, C. Pannecouque, J. Balzarini, E. De Clercq, X. Liu, Synthesis and biological evaluation of pyridazine derivatives as novel HIV-1 NNRTIs, Bioorg. Med. Chem., 21 (2013) 2128-2134.

[18] W. Chen, P. Zhan, D. Rai, E. De Clercq, C. Pannecouque, J. Balzarini, Z. Zhou, H. Liu, X. Liu, Discovery of 2-pyridone derivatives as potent HIV-1 NNRTIs using molecular hybridization based on crystallographic overlays, Bioorg. Med. Chem., 22 (2014) 1863-1872.

[19] T.L. Kishbaugh, Pyridines and Imidazopyridines With Medicinal Significance, Curr. Top. Med. Chem., (2016).

[20] X. Liu, Z. Liu, P. Zhan, Diaryl pyridine derivatives useful in treatment of human immunodeficiency virus (HIV) infection and their preparation, Faming Zhuanli Shenqing, CN104876860 (2015).

[21] M. Hasegawa, N. Nishigaki, Y. Washio, K. Kano, P.A. Harris, H. Sato, I. Mori, R.I. West, M. Shibahara, H. Toyoda, L. Wang, R.T. Nolte, J.M. Veal, M. Cheung, Discovery of novel benzimidazoles as potent inhibitors of TIE-2 and VEGFR-2 tyrosine kinase receptors, J. Med. Chem., 50 (2007) 4453-4470.

[22] R. Pauwels, J. Balzarini, M. Baba, R. Snoeck, D. Schols, P. Herdewijn, J. Desmyter, E. De Clercq, Rapid and automated tetrazolium-based colorimetric assay for the detection of anti-HIV compounds, J. Virol. Methods, 20 (1988) 309-321.

[23] C. Pannecouque, D. Daelemans, E. De Clercq, Tetrazolium-based colorimetric assay for the detection of HIV replication inhibitors: revisited 20 years later, Nat. Protoc., 3 (2008) 427-434.

[24] P. Zhan, X. Liu, Z. Li, Z. Fang, Z. Li, D. Wang, C. Pannecouque, E.D. Clercq, Novel 1,2,3-thiadiazole derivatives as HIV-1 NNRTIs with improved potency: Synthesis and preliminary SAR studies, Bioorg. Med. Chem., 17 (2009) 5920-5927.

[25] J. Auwerx, T.W. North, B.D. Preston, G.J. Klarmann, E. De Clercq, J. Balzarini, Chimeric human immunodeficiency virus type 1 and feline immunodeficiency virus reverse transcriptases: role of the subunits in resistance/sensitivity to non-nucleoside reverse transcriptase inhibitors, Mol. Pharmacol., 61 (2002) 400-406.

[26] V.L. Singer, L.J. Jones, S.T. Yue, R.P. Haugland, Characterization of PicoGreen reagent and development of a fluorescence-based solution assay for double-stranded DNA quantitation, Anal. Biochem., 249 (1997) 228-238.

[27] H.Q. Wu, J. Yao, Q.Q. He, W.X. Chen, F.E. Chen, C. Pannecouque, E. De Clercq, D. Daelemans, Synthesis and biological evaluation of DAPY-DPEs hybrids as non-nucleoside inhibitors of HIV-1 reverse transcriptase, Bioorg. Med. Chem., 23 (2015) 624-631.

[28] D. Kang, Z. Fang, Z. Li, B. Huang, H. Zhang, X. Lu, H. Xu, Z. Zhou, X. Ding, D. Daelemans, E. De Clercq, C. Pannecouque, P. Zhan, X. Liu, Design, Synthesis, and Evaluation of Thiophene[3,2-d]pyrimidine Derivatives as HIV-1 Non-nucleoside Reverse Transcriptase Inhibitors with Significantly Improved Drug Resistance Profiles, J. Med. Chem., 59 (2016) 7991-8007.

[29] M. Popovic, M.G. Sarngadharan, E. Read, R.C. Gallo, Detection, isolation, and continuous production of cytopathic retroviruses (HTLV-III) from patients with AIDS and pre-AIDS, Science, 224 (1984) 497-500.

[30] F. Clavel, D. Guetard, F. Brun-Vezinet, S. Chamaret, M.A. Rey, M.O. Santos-Ferreira, A.G. Laurent, C. Dauguet, C. Katlama, C. Rouzioux, et al., Isolation of a new human retrovirus from West African patients with AIDS, Science, 233 (1986) 343-346.

Highlights

1. Twenty-one 3,5-diaryl-pyridine derivatives were designed, synthesized and evaluated for their anti-HIV activities.
2. **5b2** (EC_{50} = 0.04 μM, SI = 3963) was the most potent inhibitor.
3. The 2-NH_2 pyridine derivatives showed better anti-HIV-1 activity than the corresponding 2-NO_2 counterparts.